



ELSEVIER

Available online at www.sciencedirect.com

SCIENCE @ DIRECT®

Physics Letters A 338 (2005) 239–246

PHYSICS LETTERS A

www.elsevier.com/locate/pla

Existence and stability analysis of solitary waves in a tricrystal junction

H. Susanto*, S.A. van Gils

Department of Applied Mathematics, University of Twente, P.O. Box 217, 7500 AE Enschede, The Netherlands

Received 9 April 2004; accepted 23 February 2005

Available online 11 March 2005

Communicated by A.R. Bishop

Abstract

We consider a tricrystal junction, i.e., a system of three long Josephson junctions coupled at a common end point. The system admits solitary waves sitting at or near the common point. Especially when one of the junctions is a π -junction, there is a solitary wave created at the branch point. The stability and the dynamics of all existing solitary waves of the time-independent system are studied analytically and numerically. The present study is of interest also for experimentalists since the system is a base for a network of transmission lines.

© 2005 Elsevier B.V. All rights reserved.

PACS: 74.50.+r; 85.25.Cp; 74.20.Rp

Keywords: Long Josephson junctions; Sine-Gordon equation; Fluxons; Tricrystal junctions

1. Introduction

One attractive application of Josephson junctions among others is their applicability for logic devices based on the Josephson effect for high-performance computers [1–3]. Employing flux quanta as information bits, the method is based on manipulating the properties, e.g., the stability, of fluxons. Nakajima, Onodera and Ogawa [2] proposed a network of Josephson junctions that is made by several junctions

connected to an overall coupling at a point. The circuits allow one to control the behavior of Josephson vortices to achieve a complete logic capability [2,3]. One of the circuits is named STP (selective turning point) where a moving integer fluxon can be trapped at the branch point (turning point).

Later, it is discussed in [5,6] that the STP equation can be used to describe an edge dislocation formed by an incomplete copper-oxide layer. The situation can be realized during the preparation of a stacked system. The authors show that a trapped vortex at the branch point executes harmonic oscillations around the equilibrium position.

* Corresponding author.

E-mail address: h.susanto@math.utwente.nl (H. Susanto).

Recently, Kogan, Clem and Kirtley [4] consider Josephson vortices at tricrystal boundaries. It is interesting to see that this tricrystal problem is also described by the same equation as the above-mentioned STP circuit. In [4], the presence of a half-integer flux is discussed when one of the three Josephson junctions is a π -junction, i.e., a junction that has a phase-jump of π in the phase-difference. In advance, they consider also the existence of a state with multiple fluxes in tricrystal junctions.

In this Letter we will calculate analytically the stability of solitary waves admitted by a tricrystal junction. Knowing the eigenvalues of a state is of importance in experiments. In the time-independent case, a static solitary wave can be sitting at or near the branch (turning) point of a tricrystal junction depending on the combination of the Josephson lengths. We will consider a general case when the Josephson lengths of the junctions λ_J 's are not the same. The present work is organized in the following way. In Section 2 we will recall the governing equations as derived in [2–4]. In Section 3 we discuss the stability of integer fluxons sitting at or near the branch point. This section consists of two parts, respectively discussing one and two vortices sitting at or near the branch point. The case when one junction is a π -junction is discussed in Section 4. The conclusion of the Letter is given in Section 5.

2. Mathematical model

The time-dependent governing equation of the phase difference along the junctions is described by the following perturbed sine-Gordon equation [2,3]

$$\lambda_i^2 \phi_{xx}^i - \phi_{tt}^i = \theta^i \sin \phi^i, \quad (1)$$

with $i = 1, 2, 3$, $x > 0$, $t > 0$. The common end point is positioned at $x = 0$. λ_i is the Josephson length of the i th junction. The subscript J of the Josephson length is omitted for brevity. The index i numbers the junction. The constant parameter θ^i represents the type of the i th junction, i.e., $\theta^i = 1(-1)$ when the junction is a conventional (π -) junction. The overall coupling boundary conditions at the intersection are

$$\begin{aligned} \phi^1 + \phi^2 + \phi^3 &= 0, \\ \phi_x^1 &= \phi_x^2 = \phi_x^3, \end{aligned} \quad (2)$$

all evaluated at $x = 0$.

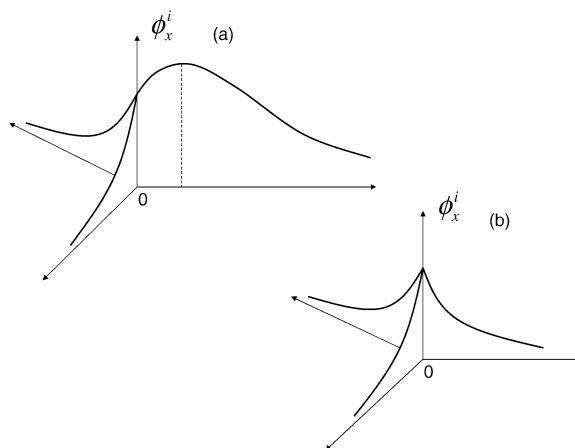


Fig. 1. A sketch of two possible field distributions ϕ_x^i of a static solitary wave at the tricrystal junction, i.e., (a) a solitary wave sitting *outside* the intersection and (b) a solitary wave sitting *at* the intersection.

The total Hamiltonian energy of Eq. (1) is given by [4]

$$H = \sum_i \int_0^\infty \left[\frac{1}{2} (\lambda_i \phi_x^i)^2 + \theta^i (1 - \cos \phi^i) \right] dx. \quad (3)$$

In this Letter we consider the time-independent solution of (1). There are several possible states for a static solitary wave admitted by (1). Two of them are sketched in Fig. 1. The configuration of the state is determined by the Josephson length of the junctions. Substituting a given time-independent solitary wave to (1) will reveal the stability of the solution. Here we will calculate the linear stability analytically.

3. Conventional tricrystal junctions

3.1. Stability of a standing integer fluxon

The first case that we will consider is a conventional tricrystal junction. A conventional junction is represented by $\theta^i = 1$ in (1). A fluxon moving in a conventional tricrystal junction through the branch point can be either trapped, bouched or passing through the point. This is the operation of a tricrystal junction as a logic gate proposed in [2,3]. In Fig. 2 a sketch of fluxon trapping is shown. We see also the oscillation of the trapped fluxon. Therefore it is clear that the branch

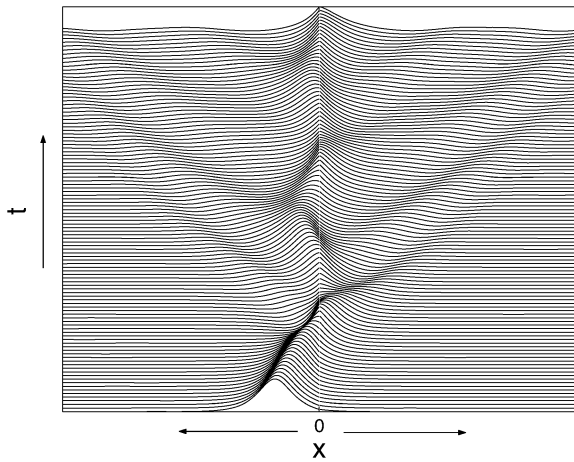


Fig. 2. A sketch of a fluxon moving with velocity 0.5 toward $x = 0$ that is trapped at the branch-point. The plot is made in terms of the magnetic field ϕ_x^i . In the sketch, to the left and to the right of $x = 0$ is junction 1 and 2, respectively. When $\lambda_2 = \lambda_3$, $\phi^2 = \phi^3$. The parameter values we take are $\lambda_1 = \lambda_2 = \lambda_3$. The release of scattered-waves can be seen as well.

point acts as a potential well. The oscillation frequency has been calculated in [6].

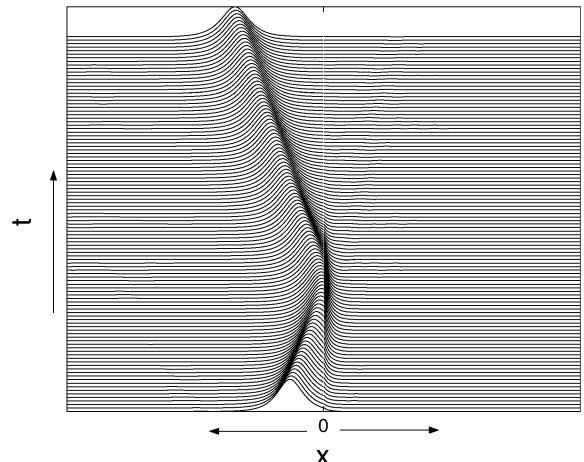
In the passing and bouncing case, an incoming fluxon will pass and be reflected by the branch point, respectively. All the cases are determined by the values of the Josephson lengths. The latter case is sketched in Fig. 3.

It is of interest to know combinations of Josephson length values that will give a particular case. In this Letter, we will assume that the incoming fluxon moves with an infinitesimal velocity. In this case we only need to consider the linear stability of a time-independent solitary wave admitted by Eq. (1). We will identify which combinations lead to trapping of a fluxon. If a static solitary wave is stable, then it is an indication that a moving fluxon will be trapped by the branch point.

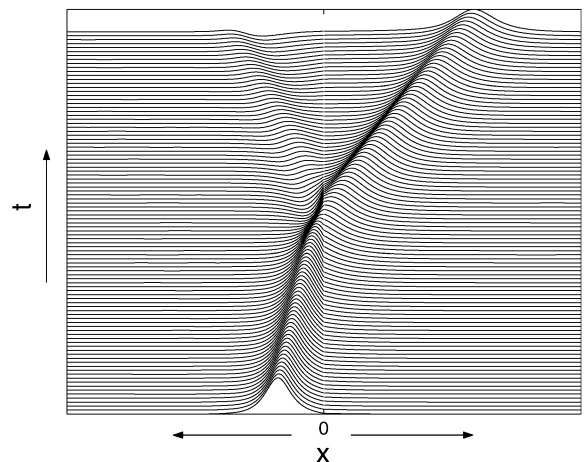
A static solution of Eq. (1) representing a fluxon sitting near the branch point is given by [4]

$$\begin{aligned} \phi_0^1 &= 4 \tan^{-1} (e^{(x-x_1)/\lambda_1}), \\ \phi_0^2 &= 4 \tan^{-1} (e^{(x-x_2)/\lambda_2}) - 2\pi, \\ \phi_0^3 &= 4 \tan^{-1} (e^{(x-x_3)/\lambda_3}) - 2\pi, \end{aligned} \quad (4)$$

where the x_i are determined by (2). For simplicity we scale the Josephson lengths to $\sum \lambda_i = 1$ such that in the calculation we need to consider only λ_i from 0 to 1.



(a)



(b)

Fig. 3. The same sketch as Fig. 2, but in the bouncing (a) and passing (b) case. The parameter values we take are (a) $\lambda_1 = 1$ and $\lambda_2 = \lambda_3 = 0.4$ and (b) $\lambda_2 = 1$, $\lambda_2 = 2$ and $\lambda_3 = 0.5$. The bounc and the passing of a 2π -kink can be an indication of the instability of a time-independent solitary wave admitted by (1) at the same parameter values.

Expression (4) does indeed represent a 2π -kink because the total Josephson phase is 2π when one circles the branch point at large distances, i.e., $\sum_i \phi_0^i(\infty) = 2\pi$.

First we will derive $x_i = x_i(\lambda_2, \lambda_3)$. The procedure we will write below is a summary of the steps given in [4].

Substituting (4) into (2) gives the following equations:

$$\begin{aligned} \gamma_i \eta &= \sin 2\alpha_i, \quad i = 2, 3, \\ \alpha_3 &= \pi - \alpha_1 - \alpha_2, \end{aligned} \tag{5}$$

where

$$\begin{aligned} \gamma_i &= \lambda_i / \lambda_1, \quad \eta = \sin 2\alpha_1, \\ \alpha_i &= \tan^{-1}(e^{-x_i / \lambda_i}). \end{aligned} \tag{6}$$

Manipulating the last equation of (5) gives the following equation for η :

$$\gamma_3 \eta = \eta \sqrt{1 - (\gamma_2 \eta)^2} + \gamma_2 \eta \sqrt{1 - \eta^2}. \tag{7}$$

This equation has a positive root $0 < \eta < 1$ that is given by

$$\eta = \frac{\sqrt{-1 + 2(\gamma_2^2 + \gamma_3^2 + \gamma_2^2 \gamma_3^2) - \gamma_2^4 - \gamma_3^4}}{2\gamma_2 \gamma_3}. \tag{8}$$

The above η is real provided positive expression in the square root. When η is nonreal, x_i 's will also be non-real. Hence, there is no static solution representing a fluxon sitting at the branch point. In this case a moving fluxon can be either bounced or passing as shown in Fig. 3.

Once we know the value of η for given values of λ_2 and λ_3 , we can calculate x_i from $\gamma_i \eta = \sin 2\alpha_i = 1 / \cosh(x_i / \lambda_i)$, i.e.,

$$e^{x_i / \lambda_i} = \frac{1 \pm \sqrt{1 - \gamma_i^2 \eta^2}}{\gamma_i \eta}. \tag{9}$$

The minus and positive sign corresponds to $x_i < 0$ and $x_i > 0$, respectively. If one of the x_i 's is positive, then the configuration of the magnetic field will be as Fig. 1(a). Solutions that satisfy the governing equation have certain combinations of the signs of x_i .

Next, we can proceed with the stability analysis to the static solitary wave. First, we linearize about the solution ϕ_0^i . We write $\phi^i(x, t) = \phi_0^i + u^i(x, t)$ and substitute the spectral ansatz $u^i = e^{\omega t} v^i(x)$. Retaining the terms linear in u^i gives the following eigenvalue problem

$$\lambda_i^2 v_{xx}^i - (\omega^2 + \theta^i \cos \phi_0^i) v^i = 0, \tag{10}$$

with boundary conditions at $x = 0$ given by

$$\begin{aligned} v^1 + v^2 + v^3 &= 0, \\ v_x^1 &= v_x^2 = v_x^3. \end{aligned} \tag{11}$$

The spectrum ω consists of the essential spectrum and the point spectrum (isolated eigenvalues). The essential spectrum is given by those ω for which there exist a solution to

$$\lambda_i^2 v_{xx}^i - [\omega^2 + (\lim_{x \rightarrow \infty} \theta^i \cos \phi_0^i)] v^i = 0,$$

i.e.,

$$\lambda_i^2 v_{xx}^i - (\omega^2 + 1) v^i = 0 \tag{12}$$

of the form $v^i = e^{i\kappa x / \lambda_i}$, with κ real.

It follows that

$$\omega = \frac{\pm \sqrt{-4(1 + \kappa^2)}}{2}. \tag{13}$$

This relation is the usual dispersion relation of a linear wave in a sine-Gordon equation. This relation forms a semi-infinite continuous spectrum in the imaginary axis.

The above stability analysis shows that solution (4) can be stable. We cannot conclude whether the solution is linearly stable or not before analyzing the point spectrum.

Our next task is to find the point spectrum ω and the corresponding eigenfunction v^i . The point spectrum consists of those value of ω for which there exist solutions v^i to (10), (11) that converge to 0 at $x = \infty$.

The eigenfunction v^i that corresponds to the eigenvalue is of the form [7,8]

$$v^i(x) = c_i e^{\mu \frac{x-x_i}{\lambda_i}} \left(\tanh \frac{x-x_i}{\lambda_i} - \mu \right), \quad \mu^2 = \omega^2 + 1, \tag{14}$$

where $\text{Re}(\mu) \leq 0$, and c_i needs to be determined from (11).

To obtain an expression for the eigenvalues of the fluxon state for the general case, we have a polynomial of order five in μ derived from (11) with (14). The polynomial coefficients depend on λ_i , $i = 1, 2, 3$. The obtained polynomial is presented in Appendix A.

When all the Josephson lengths are the same, $x_i = -\lambda_i \ln \sqrt{3}$. In this special case, the roots of the polynomials are

$$\mu = \frac{1}{2}, \frac{1 \pm \sqrt{13}}{4}.$$

The last two roots have multiplicity two. The eigenvalue is known by recalling that $\text{Re}(\mu) \leq 0$ and

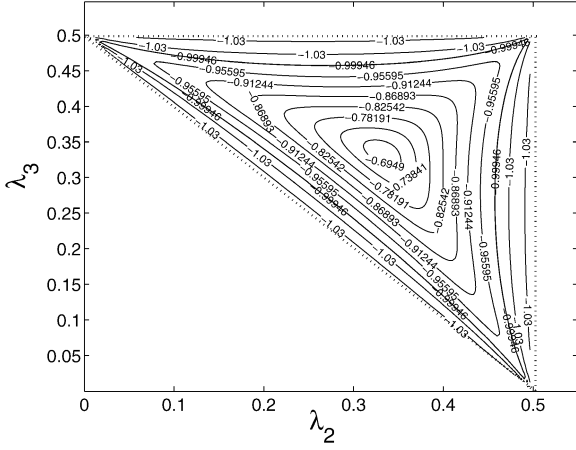


Fig. 4. The smallest spectral parameter μ for a standing 2π -fluxon. The instability corresponds to $\mu < -1$. The region outside the dotted lines gives negative values in the expression within the square root of (8). In this region, it is directly clear that there will be no trapped fluxon.

$\mu^2 = \omega^2 + 1$ from which we obtain

$$\omega = \pm i \sqrt{\frac{1 + \sqrt{13}}{8}}. \quad (15)$$

This result is in accordance with [5]. The spectral parameter μ in $\lambda_2\lambda_3$ -plane is shown in Fig. 4.

It is interesting to note that there is a region in the plane with unstable standing solitary wave ($\text{Re}(\omega) > 0$ or $\text{Re}(\mu) < -1$). In the unstable region, the magnetic field configuration is as Fig. 1(a). In this combination of parameter values, a moving fluxon through the branch point will not be trapped by the branch point.

3.2. Stability of two standing fluxons

Next we will consider the linear stability of two fluxons sitting at or near the branch point. If we can find a combination of Josephson lengths that gives a stable 4π -kink, then two incoming fluxons can be trapped at the branch point. The stability calculation can be done as before by starting that a solution corresponding to the state is given by

$$\begin{aligned} \phi_0^1 &= 4 \tan^{-1}(e^{(x-x_1)/\lambda_1}), \\ \phi_0^2 &= 4 \tan^{-1}(e^{(x-x_2)/\lambda_2}), \\ \phi_0^3 &= 4 \tan^{-1}(e^{(x-x_3)/\lambda_3}) - 2\pi. \end{aligned} \quad (16)$$

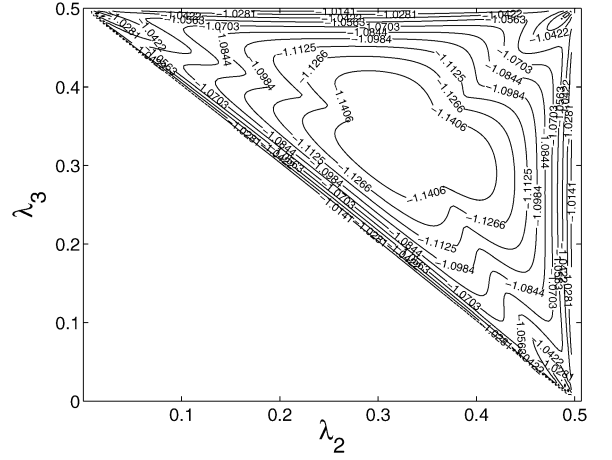


Fig. 5. The smallest spectral parameter μ for a standing 4π -fluxon. It is clear that in all regions the state is unstable. It means that there is no possibility to trap two fluxons at the branch point.

Redoing the same steps as above, one can make the spectrum parameter of a 4π -state in $\lambda_2\lambda_3$ -plane. We solved the polynomial of μ (see Appendix A) numerically. The result is shown in Fig. 5. Because the largest eigenvalue is always positive for any combination of the Josephson lengths, then no two fluxons can be trapped at the branch point.

For three standing fluxons, one can show analytically using phase-portrait analysis that there is no static three fluxons, i.e., $x_i = \pm\infty$. It is directly clear that there can be no three fluxon trapped at the branch point.

4. Tricrystal junctions with a π -junction

The next problem we would like to solve is when one of the junctions is a π -junction. This problem appears in superconducting crystals with d -wave symmetry [9]. Josephson boundaries between anisotropic superconductors with the d -wave symmetry is sensitive to crystalline misorientation. In a particular case, the phase difference can have a phase addition of π .

In the presence of a phase-jump of π in the phase difference of one junction, half-flux quantum is the ground state of the system [4]. In this case, a π -kink is *spontaneously generated* or—in mathematical terms—the global attractor of the system. Therefore, a π -kink is used also to probe the unconventional sym-

metry of a junction [10,11]. Only recently it is proposed to use half-flux quanta, but in a different system, in superconducting memory devices [12].

To describe this problem, Eq. (1) has $-\theta^1 = \theta^{2,3} = 1$. This system has a π -soliton which is the ground state. A static solution representing the state is given as

$$\begin{aligned} \phi_0^1 &= 4 \tan^{-1}(e^{(x-x_1)/\lambda_1}) - \pi, \\ \phi_0^2 &= 4 \tan^{-1}(e^{(x-x_2)/\lambda_2}) - 2\pi, \\ \phi_0^3 &= 4 \tan^{-1}(e^{(x-x_3)/\lambda_3}) - 2\pi. \end{aligned} \tag{17}$$

Further treatments can be done as before. The equation for η (see (5), (6) reads as [4]

$$\sqrt{(1-\eta^2)(1-\lambda_2^2\eta^2)} - \lambda_2\eta^2 = \lambda_3\eta. \tag{18}$$

In a special case when $\lambda_i = 1/3$, $x_i = \lambda_i \ln(2 - \sqrt{3})$. In this case the spectral parameter μ (see (14)) is given by

$$\mu = \frac{\sqrt{3} - \sqrt{7}}{4},$$

from which we obtain the following eigenvalues

$$\omega = \pm i \frac{3 + \sqrt{21}}{8} \approx \pm 0.9478i. \tag{19}$$

These eigenvalues have double multiplicity. For the general case, the spectral parameter μ in the $\lambda_2\lambda_3$ -plane is shown in Fig. 6. It is interesting to note that if a

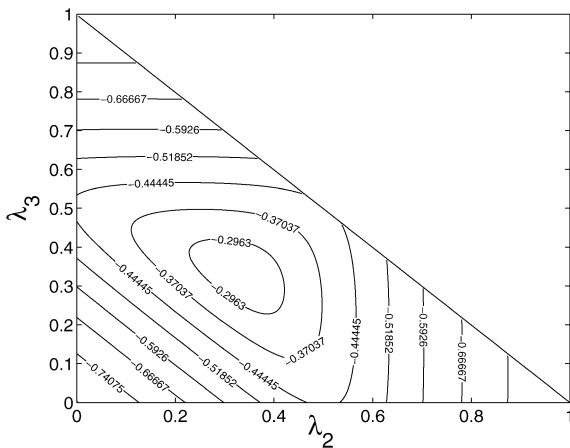


Fig. 6. The smallest spectral parameter μ for a π -fluxon. It is clear that in all regions the state is stable. The region above the line $\lambda_2 + \lambda_3 = 1$ is not a physical region since in this region $\lambda_1 < 0$ due to our scaling $\sum \lambda_i = 1$.

tricrystal junction has a π -junction, then the π -fluxon is always stable for any combinations of Josephson lengths. Under certain conditions, a π -fluxon is always observed in experiments [9–11].

Kogan, Clem and Kirtley [4] consider also the presence of $(2n + 1)\pi$ -fluxon in system (1) with $n = 0, 1, 2$. This state is rather interesting since in some combinations of the Josephson lengths, a 3π -fluxon has a lower Hamiltonian energy than a π -fluxon at the branch point and a 2π -fluxon at infinity [4]. Later on it is shown in [13] that a 3π -fluxon is unstable. Only with some combinations we can have a marginally sta-

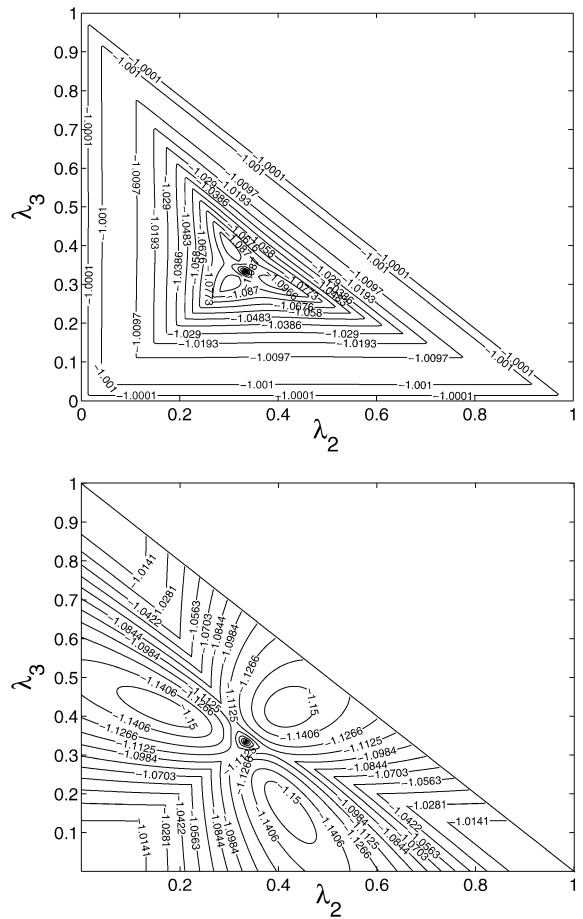
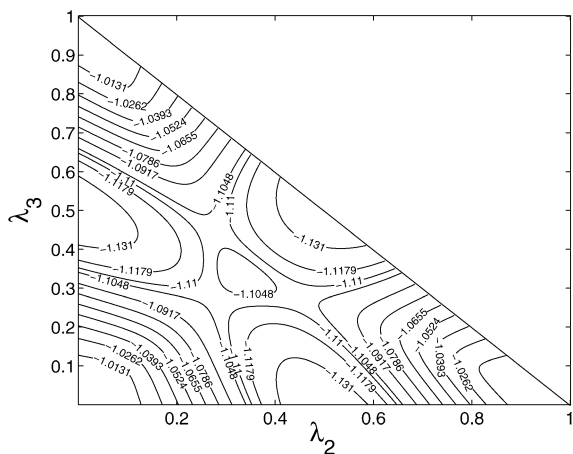


Fig. 7. The same pictures as Fig. 6 but for a 3π -fluxon with (upper) one positive x_i and (lower) two positive x_i 's. The standing state is sitting outside the branch. A 3π -kink is marginally stable when $\mu = -1$. From the picture we know that this value is attained only at unphysical combinations of Josephson lengths, for instance, when $\lambda_i = 1/3$.



$$\begin{aligned}
A_3 &= -2 \cosh\left(\frac{x_1}{\lambda_1}\right)^2 \cosh\left(\frac{x_3}{\lambda_3}\right)^2 \\
&\quad + 3 \sinh\left(\frac{x_2}{\lambda_2}\right) \sinh\left(\frac{x_3}{\lambda_3}\right) \\
&\quad \times \cosh\left(\frac{x_1}{\lambda_1}\right)^2 \cosh\left(\frac{x_2}{\lambda_2}\right) \cosh\left(\frac{x_3}{\lambda_3}\right) \\
&\quad + 3 \sinh\left(\frac{x_2}{\lambda_2}\right) \sinh\left(\frac{x_1}{\lambda_1}\right) \\
&\quad \times \cosh\left(\frac{x_1}{\lambda_1}\right) \cosh\left(\frac{x_2}{\lambda_2}\right) \cosh\left(\frac{x_3}{\lambda_3}\right)^2 \\
&\quad + 3 \sinh\left(\frac{x_3}{\lambda_3}\right) \sinh\left(\frac{x_1}{\lambda_1}\right) \\
&\quad \times \cosh\left(\frac{x_1}{\lambda_1}\right) \cosh\left(\frac{x_2}{\lambda_2}\right)^2 \cosh\left(\frac{x_3}{\lambda_3}\right) \\
&\quad - 2 \cosh\left(\frac{x_2}{\lambda_2}\right)^2 \cosh\left(\frac{x_3}{\lambda_3}\right)^2 \\
&\quad - 2 \cosh\left(\frac{x_1}{\lambda_1}\right)^2 \cosh\left(\frac{x_2}{\lambda_2}\right)^2, \\
A_2 &= 3 \sinh\left(\frac{x_2}{\lambda_2}\right) \sinh\left(\frac{x_3}{\lambda_3}\right) \sinh\left(\frac{x_1}{\lambda_1}\right) \\
&\quad \times \cosh\left(\frac{x_1}{\lambda_1}\right) \cosh\left(\frac{x_2}{\lambda_2}\right) \cosh\left(\frac{x_3}{\lambda_3}\right) \\
&\quad - 2 \sinh\left(\frac{x_3}{\lambda_3}\right) \cosh\left(\frac{x_2}{\lambda_2}\right)^2 \cosh\left(\frac{x_3}{\lambda_3}\right) \\
&\quad - 2 \sinh\left(\frac{x_1}{\lambda_1}\right) \cosh\left(\frac{x_1}{\lambda_1}\right) \cosh\left(\frac{x_2}{\lambda_2}\right)^2 \\
&\quad - 2 \sinh\left(\frac{x_3}{\lambda_3}\right) \cosh\left(\frac{x_1}{\lambda_1}\right)^2 \cosh\left(\frac{x_3}{\lambda_3}\right) \\
&\quad - 2 \sinh\left(\frac{x_2}{\lambda_2}\right) \cosh\left(\frac{x_2}{\lambda_2}\right) \cosh\left(\frac{x_3}{\lambda_3}\right)^2 \\
&\quad - 2 \sinh\left(\frac{x_1}{\lambda_1}\right) \cosh\left(\frac{x_1}{\lambda_1}\right) \cosh\left(\frac{x_3}{\lambda_3}\right)^2 \\
&\quad - 2 \sinh\left(\frac{x_2}{\lambda_2}\right) \cosh\left(\frac{x_1}{\lambda_1}\right)^2 \cosh\left(\frac{x_2}{\lambda_2}\right), \\
A_1 &= \cosh\left(\frac{x_1}{\lambda_1}\right)^2 + \cosh\left(\frac{x_2}{\lambda_2}\right)^2 + \cosh\left(\frac{x_3}{\lambda_3}\right)^2 \\
&\quad - 2 \sinh\left(\frac{x_2}{\lambda_2}\right) \sinh\left(\frac{x_3}{\lambda_3}\right) \cosh\left(\frac{x_2}{\lambda_2}\right) \cosh\left(\frac{x_3}{\lambda_3}\right) \\
&\quad - 2 \sinh\left(\frac{x_3}{\lambda_3}\right) \sinh\left(\frac{x_1}{\lambda_1}\right) \cosh\left(\frac{x_1}{\lambda_1}\right) \cosh\left(\frac{x_3}{\lambda_3}\right) \\
&\quad - 2 \sinh\left(\frac{x_2}{\lambda_2}\right) \sinh\left(\frac{x_1}{\lambda_1}\right) \cosh\left(\frac{x_1}{\lambda_1}\right) \cosh\left(\frac{x_2}{\lambda_2}\right),
\end{aligned}$$

$$\begin{aligned}
A_0 &= \sinh\left(\frac{x_2}{\lambda_2}\right) \cosh\left(\frac{x_2}{\lambda_2}\right) + \sinh\left(\frac{x_1}{\lambda_1}\right) \cosh\left(\frac{x_1}{\lambda_1}\right) \\
&\quad + \sinh\left(\frac{x_3}{\lambda_3}\right) \cosh\left(\frac{x_3}{\lambda_3}\right). \tag{A.2}
\end{aligned}$$

References

- [1] P.D. Shaju, V.C. Kuriakose, *Physica C* 322 (1999) 163.
- [2] K. Nakajima, Y. Onodera, Y. Ogawa, *J. Appl. Phys.* 47 (1976) 1620.
- [3] K. Nakajima, Y. Onodera, *J. Appl. Phys.* 49 (1978) 2958.
- [4] V.G. Kogan, J.R. Clem, J.R. Kirtley, *Phys. Rev. B* 61 (2000) 9122.
- [5] A. Grunnet-Jepsen, F.N. Fahrendorf, S.A. Hattel, N. Grønbech-Jensen, M.R. Samuelsen, *Phys. Lett. A* 175 (1993) 116.
- [6] S.A. Hattel, A. Grunnet-Jepsen, M.R. Samuelsen, *Phys. Lett. A* 221 (1996) 115.
- [7] E. Mann, *J. Phys. A: Math. Gen.* 30 (1997) 1227.
- [8] G. Derks, A. Doelman, S.A. van Gils, T.P.P. Visser, *Physica D* 180 (2003) 40.
- [9] C.C. Tsuei, J.R. Kirtley, *Rev. Mod. Phys.* 72 (2000) 969.
- [10] J.R. Kirtley, C.C. Tsuei, M. Rupp, J.Z. Sun, L.S. Yu-Jahnes, A. Gupta, M.B. Ketchen, K.A. Moler, M. Bhushan, *Phys. Rev. Lett.* 76 (1996) 1336.
- [11] C.C. Tsuei, J.R. Kirtley, *Phys. Rev. Lett.* 85 (2000) 182.
- [12] H. Hilgenkamp, Ariando, H.J.H. Smilde, D.H.A. Blank, G. Rijnders, H. Rogalla, J.R. Kirtley, C.C. Tsuei, *Nature* 422 (2003) 50.
- [13] H. Susanto, S.A. van Gils, A. Doelman, G. Derks, *Phys. Rev. B* 69 (2004) 212503.